


SPECIAL ISSUE ARTICLE

Multivalent dextran hybrids for efficient cytosolic delivery of biomolecular cargoes

Bastian Becker¹ | Simon Englert¹ | Hendrik Schneider¹ | Desislava Yanakieva¹ | Sarah Hofmann¹ | Carolin Dombrowsky¹ | Arturo Macarrón Palacios¹ | Sebastian Bitsch¹ | Adrian Elter^{1,2} | Tobias Meckel² | Benedikt Kugler³ | Anastasya Schirmacher³ | Olga Avrutina¹ | Ulf Diederichsen³ | Harald Kolmar¹ 

¹Institute for Organic Chemistry and Biochemistry, Technical University of Darmstadt, Alarich-Weiss-Straße 4, Darmstadt, 64287, Germany

²Merck Lab, Technische Universität Darmstadt, Alarich-Weiss-Straße 8, Darmstadt, 64287, Germany

³Institute for Organic and Biomolecular Chemistry, Georg-August-Universität Göttingen, Tammannstraße 2, Göttingen, 37077, Germany

Correspondence

Harald Kolmar, Institute for Organic Chemistry and Biochemistry, Technical University of Darmstadt, Alarich-Weiss-Straße 4, Darmstadt 64287, Germany.
Email: kolmar@biochemie-tud.de

Funding information

Deutsche Forschungsgemeinschaft, Grant/Award Number: SPP1623

The development of novel biotherapeutics based on peptides and proteins is often limited to extracellular targets, because these molecules are not able to reach the cytosol. In recent years, several approaches were proposed to overcome this limitation. A plethora of cell-penetrating peptides (CPPs) was developed for cytoplasmic delivery of cell-impermeable cargo molecules. For many CPPs, multimerization or multicopy arrangement on a scaffold resulted in improved delivery but also higher cytotoxicity. Recently, we introduced dextran as multivalent, hydrophilic polysaccharide scaffold for multimerization of cell-targeting cargoes. Here, we investigated covalent conjugation of a CPP to dextran in multiple copies and assessed the ability of resulted molecular hybrid to enter the cytoplasm of mammalian cells without largely compromising cell viability. As a CPP, we used a novel, low-toxic cationic amphiphilic peptide L17E derived from M-lycotoxin. Here, we show that cell-penetrating properties of L17E are retained upon multivalent covalent linkage to dextran. Dextran-L17E efficiently mediated cytoplasmic translocation of an attached functional peptide and a peptide nucleic acid (PNA). Moreover, a synthetic route was established to mask the lysine side chains of L17E with a photolabile protecting group thus opening avenues for light-triggered activation of cellular uptake.

KEYWORDS

cell penetrating peptide, intracellular delivery, multimerization, oligosaccharides, peptide nucleic acids, peptides

1 | INTRODUCTION

The last few decades have seen increasing interest in the development of novel therapeutics based on biologicals, among them peptides.¹ With their beneficial properties like high potency and

specificity,² these structurally complex architectures have been reported to modulate certain cellular processes with high specificity and efficacy.³ However, the action of biopharmaceuticals is often limited to extracellular targets as these molecules are not able to enter the cytosol, which drastically narrows their potential application field.⁴ A number of strategies have been developed to date to overcome this obstacle by improving cellular uptake, among them noncovalent

Bastian Becker and Simon Englert contributed equally to this work.

This is an open access article under the terms of the Creative Commons Attribution-NonCommercial License, which permits use, distribution and reproduction in any medium, provided the original work is properly cited and is not used for commercial purposes.

© 2021 The Authors. *Journal of Peptide Science* published by European Peptide Society and John Wiley & Sons Ltd.

delivery with liposomes⁵ and nanoparticles⁶ and transport with diselenolanes⁷ or cell-penetrating peptides (CPPs).

Comprising oligopeptides of cationic and/or amphipathic nature,⁸ CPPs have recently emerged as efficient vehicles ensuring cellular delivery of various cargoes, among them peptides^{9,10} and proteins,^{11,12} following different mechanisms that depend on their structural peculiarities (for the details of those mechanisms, see Ruseska and Zimmer⁸ and Dougherty et al.¹³). Electrostatic interactions with the cellular membrane induce cell entrance of CPPs either via direct translocation or by different pathways of endocytosis, or both.⁸ If the endocytic uptake mechanism prevails, cargo molecules are entrapped in the endosome and prone to subsequent lysosomal degradation. As a consequence, endosomal escape is strictly required to release the cargo into the cytosol.^{4,14} Not only CPPs¹⁵ but also other drug delivery systems suffer from endosomal entrapment as well^{4,14}; therefore, escape strategies like the use of pH-sensitive endosomal membrane-perturbing peptides have been employed to overcome this issue.^{16–18}

A plethora of CPPs have been developed, most of them containing a large fraction of arginines. It has been shown¹⁹ that cyclization of oligoarginines enhances direct cytoplasmic uptake; additionally, efforts were made to identify efficient CPPs by application of synthetic molecular evolution methods.⁹ Besides, arginine-rich cationic peptides and amphipathic and hydrophobic ones have been reported, with their uptake mechanisms remaining largely unknown²⁰ and depending on cargo, cell types, and concentration, as well as incubation temperature and time.^{20,21} A subclass of these arginine-free CPPs has been recently described by Futaki and coworkers.¹⁶ Starting with M-lycotoxin, a haemolytic peptide from the wolf spider *Lycosa carolinensis*,²² they replaced certain amino acids at the potential hydrophobic face with glutamic acid in order to diminish the lytic activity at physiological pH by preventing hydrophobic interactions with the cellular membrane. As a result, the most promising variant L17E displayed strongly reduced cytotoxicity (more than 30-fold compared to the parent M-lycotoxin) and promoted cytoplasmic delivery of functional proteins like Cre recombinase and antibodies (IgG) upon cocubation.¹⁶ Futaki and coworkers proposed a novel major uptake pathway by transient membrane permeabilization. Thus, interaction of L17E with the cell membrane is thought to induce its ruffling by actin rearrangement, ultimately leading to macropinocytosis. Before the formation of the macropinosome is completed, L17E presumably ruptures the ruffled membrane, thus allowing macromolecules to directly enter the cytoplasm.²³ Besides mechanistic features of cell internalization, this type of delivery peptide is particularly interesting since, due to presence of five lysines, it provides the option of chemically masking the lysine side chains using well-known photolabile protecting groups,^{24,25} so that conceptually cytoplasmic delivery could be triggered by light.

Delivery of cargoes via CPPs in most applications occurs via cocubation or upon covalent linkage of the CPP to the cargo molecule.²⁶ It has been previously demonstrated that some CPPs like arginine-rich TAT peptide or arginine-lacking transportan 10 displayed higher cellular uptake propensity when presented in multiple copies

on a branched dendrimer, however, often at the cost of enhanced cytotoxicity.²⁷ For the M-lycotoxin L17E variant (abbreviated L17E in the following), no efforts were made yet to covalently link transporter peptide and cargo, and only cocubation experiments were described.

In this work, we intended to establish a modular approach for cytoplasmic delivery of peptides and peptide nucleic acids via conjugation to dextran polymer (Scheme 1) without largely compromising cell viability using the L17E transporter. This would allow for the easy variation of CPP-to-cargo proportion simply by adjusting their molar ratio upon dextran conjugation, aimed at finding an optimal balance between efficient cargo delivery and cytotoxicity. Indeed, nonaarginine (R9)-functionalized dextran was shown to deliver a proapoptotic peptide into the cytoplasm of human Jurkat cells.²⁸ However, further analysis of the R9-dextran conjugates revealed that the constructs exhibited strongly increased cytotoxicity compared to solitary R9.²⁹ Here, we describe the synthesis of dextran conjugates with CPP L17E and assess cytotoxicity of the hybrid construct. We examined cell-penetration with the help of dextran-L17E hybrids and observed efficient delivery of the fluorescent dye TAMRA, a GFP fluorescence complementing peptide GFP11, and a peptide nucleic acid that inhibits mRNA mis-splicing in cell nucleus resulting in restoration of GFP synthesis. We furthermore established a synthesis route towards derivatives of L17E bearing photocleavable protecting groups.

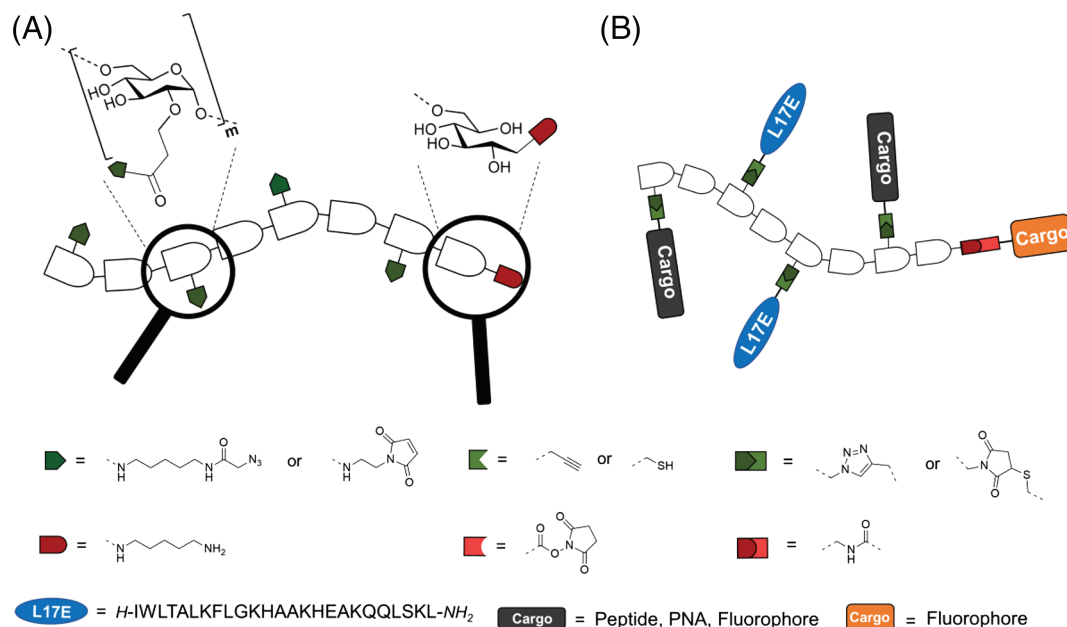
2 | MATERIALS AND METHODS

2.1 | Materials

All reagents and solvents were purchased from Agilent Technologies, Carbolution, Fisher Scientific, Iris Biotech, Jena Bioscience, Roth, Acros Organics, PNA Bio Inc., or Sigma Aldrich and used without further purification, unless stated otherwise. Anhydrous dimethyl sulfoxide (DMSO) and dichloromethane (DCM) were purchased from Acros Organics (Fair Lawn, NJ, USA). *N,N*-diisopropylethylamine (DIEA) was dried by addition of 25 g × L⁻¹ calcium hydride and stirring for 3 h at reflux, followed by vacuum distillation. Boc-cadaverine, cadaverine, and dextran from *Leuconostoc mesenteroides* (average mol. mass 9,000–11,000; minimal branching of ~5%. $M_w = 10,480 \text{ g} \times \text{mol}^{-1}$), *N*-ethoxycarbonyl-2-ethoxy-1,2-dihydroquinoline (EEDQ), and 2-azidoacetic acid were purchased from Sigma-Aldrich (Taufkirchen, Germany). From Jena Bioscience (Jena, Germany), 2-(4-((bis(1-(tert-butyl)-1H-1,2,3-triazol-4-yl)methyl)amino)methyl)-1H-1,2,3-triazol-1-yl) acetic acid (BTAA) was purchased. PNA building blocks were acquired by PNA Bio Inc. (Newbury Park, CA, USA).

2.2 | Solid-phase peptide synthesis

All peptides were synthesized using Fmoc-based solid-phase peptide synthesis on *AmphiSpheres 40* RAM resin (0.34 mmol/g) from Agilent



SCHEME 1 (A) Depiction of dextran bearing orthogonal chemical handles at the repeating units (dark green) and reducing end (dark red) with their respective counterparts (light green and light red) and consequent conjugation products. (B) Setup of dextran as delivery module with both cargo and L17E at the repeating units and a second cargo at the reducing end

Technologies (Waldbronn, Germany) or on 2-chlorotrityl chloride resin (1.6 mmol/g) from *Iris Biotech* (Marktredwitz, Germany). For fully automated microwave-assisted synthesis, a CEM (Kamp-Lintfort, Germany) *Liberty blue*® platform was applied at a 0.25 mmol scale. Coupling of amino acids was based on the *N,N*-disopropylcarbodiimide (DIC)/ethyl-2-cyano-2-(hydroxyimino) acetate (Oxyma, Iris-Biotech) activation system, and *N*-terminal Fmoc was deprotected using 20% (v/v) piperidine and 0.1 M Oxyma in *N,N*-dimethylformamide (DMF). As required, amino acids were protected according to a standard Fmoc/*tert*-butyl scheme. When manual Fmoc-SPPS was performed, 1-[bis(dimethylamino)methylene]-1H-1,2,3-triazolo[4,5-b]pyridinium 3-oxide hexafluorophosphate (HATU, Carbolution) and *N,N*-diisopropylethylamine (DIEA) activation system and 20% piperidine in DMF deprotection were applied.

2.3 | RP-HPLC

Peptides were analyzed using either an Agilent 1100 device equipped with an *Agilent Eclipse Plus* RP column (C18, 100 × 4.6 mm, 3.5 μm, 95 Å) or an *Agilent Infinity 1260* device equipped with an *Interchim* (Montluçon, France) *Uptisphere Strategy* RP column (C18-HQ, 3 μm, 100 × 4.6 mm) at a flow rate of 0.6 ml min⁻¹. Alternatively, analytical HPLC measurements were performed on an *UltiMate 3000* system from *Thermo Fisher Scientific GmbH* and an *ACE*® (Aberdeen, Scotland) *Excel*® 2 C18-100 (100 × 2.1 mm, 2 μm) column at a flow rate of 0.45 ml × min⁻¹ and 50°C. Linear gradients of eluent A (water +0.1%

trifluoroacetic acid [TFA]) and eluent B (MeCN + 0.1% TFA) in 15 min were applied.

Peptides were purified on a semipreparative RP-HPLC *Interchim Puriflash* 4250 equipped with a semipreparative C18 RP column (*Interchim Uptisphere Strategy*; C18-HQ, 5 μm, 250 × 21.2 mm). At a flow rate of 18 ml × min⁻¹, 5 min of isocratic flow (starting concentration of eluent B) was followed by 20 min of gradient flow: eluent A, 0.1% (v/v) aq. TFA; eluent B, 90% (v/v) aq. MeCN with 0.1% (v/v) TFA. Absorption was detected at 220 and 280 nm. Or purification was performed using a *JASCO* (Tokyo, Japan) system (pumps *PU-4086*, detector *UV-4075*, and column oven *CO-4060*) with an *ACE*® (Aberdeen, Scotland) 5 C18-100 (150 × 21.2 mm, 5 μm, flow rate 10 ml × min⁻¹) or *Ace*® (Aberdeen, Scotland) 5 C18-300 (150 × 10 mm, 5 μm, flow rate 3 ml × min⁻¹) at 50°C. Aliquots of the crude peptide (10 mg) were dissolved in 1,1,1,3,3,3-hexafluoroisopropanol (HFIP) (100 μl) and diluted with water (400 μl) prior to injection and filtered. Linear gradients of A (water +0.1% TFA) and B (MeOH + 0.1% TFA) in 30 min were used. Chromatograms were recorded at 215 and 280 nm.

2.4 | SEC-HPLC

Dextran derivatives were analyzed on a *Phenomenex* (Aschaffenburg, Germany) *BioSep SEC-s2000* column using an *Agilent 1100* device at a flow rate of 0.6 ml × min⁻¹. Same eluents as for RP-HPLC were used, and samples were eluted at an isocratic flow of 30% eluent B.

2.5 | Mass spectrometry

Electrospray ionization mass spectrometry (ESI-MS) spectra were obtained using a Shimadzu (Kyoto, Japan) LCMS-2020 mass spectrometer equipped with a Phenomenex Synergy 4 u Fusion-RP 80 (C-18, 250 × 4.6 mm, 2 μm, 80 Å). Eluent system consisted of 0.1% (v/v) aq. formic acid (FA; LC-MS grade, Fisher Scientific; Hampton, NH, USA; eluent A) and acetonitrile containing 0.1% (v/v) FA (LC-MS grade; eluent B).

Alternatively, LC-MS spectra were recorded on an UltiMate 3000 system from Thermo Fisher Scientific GmbH and an ACE® Excel® 2 C18-100 (100 × 2.1 mm, 2 μm) column at a flow rate of 0.45 ml × min⁻¹ and 50°C using a linear gradient of 10% A (water +0.1% FA) to 95% B (MeCN +0.1% FA) in 15 min, coupled to an LTQ XL ion trap spectrometer from Thermo Fisher Scientific GmbH (Waltham, MA, USA). Chromatograms were monitored at wavelengths of 215, 280, and 380 nm. Electrospray ionization (ESI-HRMS) spectra were recorded on a maXis (ESI-QTOF-MS) or a micrOTOF (ESI-TOF-MS with HPLC [Agilent 1200 series]) device from Bruker Daltonik GmbH (Billerica, MA, USA).

2.6 | NMR spectroscopy

NMR measurements were recorded on an Avance III or an Avance II NMR Spectrometer at 300 MHz (Bruker BioSpin GmbH, Rheinstetten, Germany) or on a Bruker Avance Neo 600 (600 MHz). ¹³C NMR was performed on a Bruker Avance Neo 600 (150 MHz). Samples were dissolved in deuterium oxide, CDCl₃, or DMSO-d₆ from Sigma Aldrich.

2.7 | IR spectroscopy

IR measurements were performed using homogenous potassium bromide pellet or by attenuated total reflection (ATR)-IR on a FTIR-Spectrometer Spectrum Two (PerkinElmer, Rodgau, Germany). Spectra were obtained by PerkinElmer Spectrum following instructions of manufacturer: wave number area, 8.300–350 cm⁻¹; spectral solution, 0.5 cm⁻¹; wave number accuracy better than 0.01 cm⁻¹ at 3.000 cm⁻¹; wave number correctness, 0.1 cm⁻¹ at 3.000 cm⁻¹; signal-to-noise ratio, 9.300: one peak to peak, 5 s, and 32.000: one peak to peak, 1 min.

2.8 | UV/Vis spectroscopy

UV/Vis-spectroscopy was performed on a Shimadzu UVmini 1240 device using Hellma (Müllheim, Germany) Quartz SUPRASIL® cuvettes.

2.9 | Thin-layer chromatography and column chromatography

Thin-layer chromatography (TLC) analysis was performed on aluminum TLC plates with silica gel 60 F₂₄₅ from Merck KGaA. Compounds

were detected by fluorescence quenching with UV-light (λ = 254 nm) or via fluorescence (λ_{ex} = 366 nm). Column chromatography was performed on Geduran® silica gel 60 (40–63 μm), supplied by Merck KGaA.

2.10 | Synthesis of S-3-tritylmercaptopropionic acid 25

The synthesis was performed as described in literature.³⁰ In anhydrous DCM, 3-Mercaptopropionic acid (1 eq.) was dissolved. Trityl chloride (1.1 eq.) in anhydrous DCM was added dropwise, and the reaction was stirred overnight at ambient temperature, whereby a colorless solid precipitated. The precipitate was filtered, washed with cold diethyl ether (3 × 50 ml), and dried in airstream, yielding 7.32 g (91%).

2.11 | Synthesis of N-Boc-ethylendiamine 10

The synthesis was performed according to literature²⁸; 1,2-ethylendiamine (1.0 eq.) was dissolved in chloroform and cooled down to 0°C. A solution of Boc-anhydride (0.1 eq.) in chloroform was added dropwise over 3 h, where after the reaction mixture was allowed to warm to room temperature overnight. The solvent was removed under reduced pressure, and the oily residue was dissolved in 2 M Na₂CO₃. The aqueous solution was extracted twice with DCM, and the organic phase was dried over MgSO₄ and evaporated, yielding 5.13 g (81%) as colorless oil.

2.12 | Synthesis of 1-((N-Boc)-2-aminoethyl) maleimide 11

The synthesis was realized as described in literature.²⁸ N-Boc-ethylendiamine **10** (1.0 eq.) and triethylamine (TEA) (1.45 eq.) were dissolved in diethyl ether and cooled down to 0°C. Maleic anhydride (1 eq.) dissolved in diethyl ether was added dropwise, where after the cooling bath was removed and the reaction was stirred for further 4 h. The formed brown precipitate was filtered and dissolved in acetone. TEA (2 eq.) was added, and the reaction was heated to reflux, followed by addition of acetic anhydride (1.5 eq.). The reaction was refluxed for 20 h, where after the solvent was removed by evaporation. The brown residue was purified by column chromatography (silica gel, n-hexane:ethyl acetate 1:1) to yield 4.02 g (52%) as colorless solid.

2.13 | Synthesis of N-(2-aminoethyl)maleimide 12

The synthesis was performed according to literature²⁸; 1-((N-Boc)-2-aminoethyl)maleimide **11** was dissolved in DCM and cooled down to 0°C. TFA was added, and the reaction was stirred for 1 h while

being allowed to reach room temperature. Afterwards, the mixture was concentrated in vacuo, and the residue was precipitated in cold diethyl ether. The suspension was filtrated and the residue washed with diethyl ether (4×) and dried in a desiccator. Purification by semipreparative HPLC yielded 2.02 g (84%) was colorless solid.

2.14 | Synthesis of *N*-(5-aminopentyl)-2-azidoacetamide 4

According to the literature,³¹ the synthesis was performed on solid support. In a syringe equipped with a frit 2-chlorotrityl chloride, resin (1.6 mmol × g⁻¹, 1.0 eq.) was swollen in DCM for 20 min and washed three times with (DCM) (10 ml). A solution of cadaverine (10 eq.) and diisopropylethylamine (DIEA) (20 eq.) in DCM (5 ml) was added, and the reaction mixture was gently agitated at ambient temperature for 2 h. After washing with DCM (6 × 10 ml), a mixture of 2-azidoacetic acid (2 eq.), Oxyma (3.3 eq.) and *N,N'*-diisopropylcarbodiimide (DIC) (3.3 eq.) in DCM (10 ml) was added, and the reaction mixture was gently agitated at ambient temperature for 18 h. After washing with DCM (6 × 10 ml) and diethyl ether (10 ml). The dried resin was treated with the cleavage cocktail TFA:triethylsilane (TES):anisol: H₂O 23:1:1:1 (5 ml) at ambient temperature for 3 h. The product was precipitated and washed in cold diethyl ether. The product was purified via semipreparative RP-HPLC, yielding 390 mg (65%).

2.15 | Synthesis of L17E 8

L17E was synthesized via automated Fmoc-SPPS on a *CEM Liberty blue*® platform in 0.25 mmol scale on *Amphispheres 40* RAM resin using DIC/Oxyma activation system and 20% piperidine/0.1 M Oxyma in DMF deprotection, according to the standard procedure of the manufacturer. Subsequent to final Fmoc-deprotection the peptide resin was washed with 6 × 10 ml DCM and 2 × 5 ml diethyl ether. Side chain deprotection as well as cleavage from the solid support was performed by treating the dried resin with a mixture consisting of TFA:anisole: TES:H₂O (47:1:1:1, v:v:v:v). After shaking for 3 h at ambient temperature, the peptide was precipitated and washed with 3 × 40 ml cold diethyl ether. Peptide was isolated by semipreparative RP-HPLC to yield 295 mg (41%) after lyophilization and analyzed with LC-ESI-MS.

2.16 | Synthesis of GFP11 24

GFP11 was synthesized via automated Fmoc-SPPS on a *CEM Liberty blue*® platform in 0.1 mmol scale on *Amphispheres 40* RAM resin using DIC/Oxyma activation system and 20% piperidine/0.1 M Oxyma in DMF deprotection, according to the standard procedure of the manufacturer. After final Fmoc-deprotection, the peptide resin was washed with 6 × 10 ml DCM and 2 × 5 ml diethyl ether. Side chain deprotection as well as cleavage from the solid support was

performed by treating half amount of the dried resin with a mixture consisting of TFA:anisole: TES:H₂O (47:1:1:1, v:v:v:v). After shaking for 3 h at ambient temperature, the peptide was precipitated and washed with 3 × 40 ml cold diethyl ether. Peptide was isolated by semipreparative RP-HPLC to yield 9 mg (5%) after lyophilization and analyzed with LC-ESI-MS.

2.17 | Synthesis of L17E-Cys 14

L17E peptide with additional C-terminal cysteine was synthesized via automated Fmoc-SPPS on a *CEM Liberty blue*® platform in 0.25 mmol scale on *Amphispheres 40* RAM resin using DIC/Oxyma activation system and 20% piperidine/0.1 M Oxyma in DMF deprotection, according to the standard procedure of the manufacturer. Subsequent to final Fmoc-deprotection, the peptide resin was washed with 6 × 10 ml DCM and 2 × 5 ml diethyl ether. Side chain deprotection as well as cleavage from the solid support was performed by treating the dried resin with a mixture consisting of TFA:anisole: TES:H₂O:DTT (46:1:1:1:1, v:v:v:v:m). After shaking for 3 h at ambient temperature, the peptide was precipitated and washed with 3 × 40 ml cold diethyl ether. Peptide was isolated by semipreparative RP-HPLC to yield 396 mg (54%) after lyophilization and analyzed with LC-ESI-MS.

2.18 | Synthesis of L17E-Pra 1

L17E peptide with additional C-terminal propargyl glycine was synthesized via manual Fmoc-SPPS in 0.25 mmol scale on *Amphispheres 40* RAM resin using HATU/DIEA activation system and 20% piperidine in DMF deprotection. Coupling steps were performed under microwave irradiation (30 W, 50°C, and 10 min), and deprotection was performed at ambient temperature (5 + 10 min). After final Fmoc-deprotection, the peptide resin was washed with 6 × 10 ml DCM and 2 × 5 ml diethyl ether. Side chain deprotection as well as cleavage from the solid support was performed by treating half amount of the dried resin with a mixture consisting of TFA:anisole: TES:H₂O (47:1:1:1, v:v:v:v). After shaking for 3 h at ambient temperature, the peptide was precipitated and washed with 3 × 40 ml cold diethyl ether. Peptide was isolated by semipreparative RP-HPLC to yield 90 mg (24%) after lyophilization and analyzed with LC-ESI-MS.

2.19 | Synthesis of alkyne-GFP11 21

GFP11 peptide was synthesized via automated Fmoc-SPPS on a *CEM Liberty blue*® platform in 0.25 mmol scale on *Amphispheres 40* RAM resin using DIC/Oxyma activation system and 20% piperidine/0.1 M Oxyma in DMF deprotection, according to the standard procedure of the manufacturer. After final Fmoc-deprotection, an *N*-terminal alkyne moiety was manually added on support, applying 4 eq. 4-pentynoic acid, 6 eq. DIC, and 6 eq. oxyma overnight. The peptide resin was washed with 6 × 10 ml DCM and 2 × 5 ml diethyl ether. Side chain

deprotection as well as cleavage from the solid support was performed by treating the dried resin with a mixture consisting of TFA:anisole: TES:H₂O (47:1:1:1, v:v:v:v). After shaking for 3 h at ambient temperature, the peptide was precipitated and washed with 3 × 40 ml cold diethyl ether. Peptide was isolated by semipreparative RP-HPLC to yield 66 mg (12%) after lyophilization and analyzed with LC-ESI-MS.

2.20 | Synthesis of L17E-3PG 34 and L17E-5PG 35

Peptides were synthesized on H-Rink amide *ChemMatrix*® resin at a 0.1 mmol scale on a *Liberty Blue* automated microwave peptide synthesizer from CEM. Synthesis was performed according to standard Fmoc/tBu-protocol using DIC and Oxyma as coupling reagents and a solution of piperidine in DMF (20% [v/v]) for Fmoc deprotection. Attachment of the amino acid building blocks was performed as double coupling, using a modified CarboMax method (5 eq. aa, 10 eq. DIC, 5 eq. Oxyma, 0.5 eq. DIEA in DMF; 1: 75°C, 170 W, 15 s; 2: 90°C, 30 W, 110 s). Milder conditions with an elongated reaction time were applied for the coupling of His (1: 25°C, 0 W, 120 s; 2: 50°C, 35 W, 480 s). Removal of the temporary protecting group was carried out under standard conditions (1: 75°C, 260 W, 15 s; 2: 90°C, 60 W, 50 s). Manual coupling was carried out for the DEACM-protected lysine building blocks in a *Discardit II*™ syringe, supplied by BD and equipped with a filter by following the subsequent general procedure. To give a 0.05 M solution, 1.5 eq. of the Fmoc-protected building block were dissolved in DMF. Added to the solution were 1.48 eq. HATU, 1.5 eq. HOAt, and 3.0 eq. DIEA, which was added to the resin. The syringe was transferred to the reaction cavity of a *Discover*® microwave synthesizer from CEM GmbH, and coupling was performed at 50°C (25 W) for 10 min. Thereafter, the resin was washed with DMF (5 × 5 ml), and the coupling step was repeated. After completion of the peptide synthesis, the resin was washed with DMF (10 × 5 ml) and DCM (10 × 5 ml) and dried in vacuo. Acidic cleavage of the peptide from the resin and simultaneous side chain deprotection was achieved by treatment with a mixture of TFA/triisopropylsilane (TIPS)/water (95:2.5:2.5 [v/v]) for 3 h. The resin was washed with two additional volumes of TFA, and the combined TFA fractions were concentrated under a nitrogen stream. The crude peptide was precipitated by addition of ice-cold diethyl ether (10 ml) and isolated by centrifugation and decantation of the supernatant. This procedure was repeated four times. The crude peptide was suspended in water and freeze-dried to give a fine yellow solid.

2.21 | Synthesis of TAMRA-thiol 15

TAMRA-Peg₂-Cys was synthesized via manual Fmoc-SPPS in 0.25 mmol scale on 2-chlorotryl chloride resin. The resin was loaded with Fmoc-Cys (Trt)-OH (4 eq. + 8 eq. DIEA), next to deprotection (20% piperidine in DMF). Fmoc-8-amino-3,6-dioxo-octanoic acid

(Fmoc-O₂Oc-OH) (1.5 eq.) was coupled using HBTU (1.4 eq.) /DIEA (3 eq.) activation. After deprotection, the N-terminus was addressed with TAMRA-NHS (1.2 eq.) and DIEA (4 eq.), and the peptide resin was gently agitated overnight. The peptide resin was washed with 6 × 10 ml DCM and 2 × 5 ml diethyl ether. Cysteine side chain deprotection as well as cleavage from the solid support was performed by treating the dried resin with a mixture consisting of TFA: TES:H₂O (48:1:1, v:v:v). After shaking for 3 h at ambient temperature, the peptide was precipitated and washed with 3 × 40 ml cold diethyl ether. The residue was dissolved in 25% (v/v) aqueous MeCN and freeze-dried, yielding 73 mg (44%) as red solid, which was used without further purification.

2.22 | Synthesis of PNA 28

PNA was synthesized via manual Fmoc-SPPS on *Amphispheres* 40 RAM resin on a 0.05 mmol scale using HATU/DIEA activation and 20% piperidine in DMF for Fmoc-deprotection. First, Fmoc-Lys (Boc)-OH (4 eq.) was coupled using 3.95 eq. HATU and 8 eq. DIEA (2 and 3 h). Afterwards, PNA synthesis was performed using 1.5 eq. Fmoc/Bhoc protected PNA building block, 1.45 eq. HATU and 3 eq. DIEA (2 × 45 min), followed by deprotection (2 min, 2 × 3 min). After coupling of three PNA building blocks, a test cleavage was performed to analyze the success of synthesis. A spatula tip of dried resin was treated with 500 µl cleavage cocktail consisting of TFA:anisole: TES: H₂O (47:1:1:1, v:v:v:v). After shaking for 1 h, the PNA was precipitated in 1.5 ml cold diethyl ether and washed twice with 1 ml cold ether. Afterwards, the PNA was analyzed with RP-HPLC and ESI-MS. After completion of the sequence, the resin was split, and half of the batch was further modified. Trityl-protected 3-mercaptopropionic acid **25** (4 eq.) was coupled using 3.95 eq. HATU and 8 eq. DIEA for 2 h. The resin was washed with DCM (5 × 10 ml) and diethyl ether (5 × 10 ml) and dried in a desiccator overnight. Cleavage from solid support as well as side chain deprotection was performed using 5 ml of the same cleavage cocktail as for test cleavages. After shaking for 2 h, the PNA was precipitated in 40 ml cold diethyl ether and washed twice with 40 ml cold ether. After drying in a desiccator, the solid was dissolved in 5% (v/v) aqueous acetic acid and freeze-dried. A total of 32 mg (25%) was yielded as slightly yellow solid and used without further purification.

2.23 | Dextran modification

Dextran modifications, as described previously by Schneider et al.,^{31,32} are well established in our laboratory. There is a stock of various 2-carboxyethyl (CE)-dextran-N-Boc-cadaverines, bearing different amounts of carboxy moieties, to choose from. Briefly, Dextran-N-Boc-cadaverine **1** was synthesized by reductive amination of the reducing end. Dextran (1.0 eq.), N-Boc-cadaverine (25 eq.), and NaBH₃CN (16 eq.) were dissolved in 0.05 M borate buffer pH 8.2, and the reaction mixture was stirred at 30°C for 72 h. The product

was precipitated and washed three times in cold methanol, dried, and purified using PD 10 desalting column following the instructions of the manufacturer. The product was obtained as white powder after lyophilization (95%). Successful conversion was determined by ^1H NMR spectroscopy as described previously.³¹ Two-CE-dextran-*N*-Boc-cadaverine was synthesized by carboxyethylation. Dextran-*N*-Boc-cadaverine (1 eq.) was dissolved in 1 M NaOH, and acrylamide (2.5 eq. per desired 2-CE-group) was added. The reaction mixture was stirred at 30°C for 24 h and further 24 h at 50°C. After neutralization with 0.1 M HCl, the product was isolated using PD 10 desalting column and obtained as white powder after lyophilization. Successful conversion and quantification of carboxyethyl groups per dextran were determined by ^1H NMR spectroscopy as described previously.³¹

As a starting material for further modifications, 2-CE-dextran-*N*-Boc-cadaverines **3**, **9**, **17**, and **26** equipped with 6.5, 4.8, 5.4, and 10.5 2-CE-groups were employed.

Maleimide-dextran-*N*-Boc-cadaverines **13** and **27** were synthesized analogously to N_3 -dextran-*N*-Boc-cadaverine synthesis as reported previously.³¹ Two-CE-dextran-*N*-Boc-cadaverine **3** and **26** bearing 6.5 and 10.5 CE-groups per dextran (1.0 eq.), respectively, was dissolved in 40% aq MeCN, and EEDQ (8.5 eq. per CE-group) in 40% aq MeCN was added. After stirring at 30°C for 1 h, *N*-(2-aminoethyl)maleimide **12** (9 eq. per CE-group) was added and the reaction mixture stirred at 30°C for 4 h. The product was isolated using PD 10 desalting column and obtained as white powder after lyophilization (32 mg, 68% **13**; 21 mg 47% **27**). Successful conversion and quantification of maleimide groups per dextran were determined by ^1H NMR spectroscopy as previously described.³¹

N_3 -dextran-*N*-Boc-cadaverines **6** and **18** were synthesized as reported previously.³¹ To that end, 2-CE-dextran-*N*-Boc-cadaverine bearing 4.8 and 5.4 CE-groups per dextran (1.0 eq.) was dissolved in 40% aq MeCN, and EEDQ (8.5 eq. per CE-group) in 40% aq MeCN was added. After stirring at 30°C for 1 h, *N*-(5-aminopentyl)-2-azidoacetamide **4** (9 eq. per CE-group) was added and the reaction mixture stirred at 30°C for 4 h. The product was isolated using PD 10 desalting column and obtained as white powder after lyophilization (22 mg, 65% **6**; 40 mg, 73% **18**; 27 mg). Successful conversion and quantification of N_3 -groups per dextran were determined by ^1H NMR spectroscopy and IR-spectroscopy as previously described.³¹ For Boc-deprotection, N_3 -dextran-*N*-Boc-cadaverines **6** and **18** were dissolved in TFA and stirred at ambient temperature for 30 min. The product was evaporated, redissolved in water, and obtained as white powder after lyophilization (20 mg, 89% **7**; 34 mg, 86% **19**; 25 mg). Quantification of deprotection was determined by ^1H NMR spectroscopy as described previously.³¹

N_3 -dextran-TAMRA **20** was synthesized by dissolving N_3 -dextran-cadaverine **19** (1.0 eq.) in anhydrous DMSO. Dry DIEA (25 eq.) was added, followed by 5(6)-TAMRA-NHS (10 eq.) in anhydrous DMSO. The dark solution was shaken over night at 25°C, followed by precipitation in methanol. Afterwards, the residue was washed with MeCN, dissolved in water, and purified via PD 10 desalting column, yielding 16 mg (64%) as red solid. Purity and TAMRA loading of the product were determined by SEC-HPLC and UV/Vis spectroscopy.

2.24 | Thiol-maleimide addition onto dextran scaffold

The respective maleimide-dextran-cadaverine **13** or **27** (1.0 eq.) was dissolved in degassed 0.1 M 2-(*N*-morpholino)ethanesulfonic acid (MES) buffer pH 6.5. A solution of (a) the respective L17E-thiol peptide **14** (1.27 eq. per maleimide group) and TAMRA-thiol **15** (0.23 eq. per maleimide group) or (b) L17E-thiol peptide (0.6 eq. per maleimide group) and PNA-thiol **28** (0.6 eq. per maleimide group) in degassed 0.1 M MES pH 6.5, 25% (v/v) MeCN was added, and the reaction mixtures stirred at ambient temperature overnight. Products were isolated using disposable PD 10 desalting columns following the instructions of the supplier and obtained as white powder after freeze drying.

2.25 | Copper-catalyzed azide-alkyne cycloaddition on dextran

A freshly prepared aqueous solution of ascorbic acid (3.2 eq. per N_3) and $\text{CuSO}_4 \cdot 5\text{H}_2\text{O}$ (1.6 eq. per N_3) was added to the solution of L17E-alkyne **1** in 25% aq MeCN (1.6 eq. per N_3). The mixture was added to the respective N_3 -dextran **7** (1.0 eq.) and stirred at 30°C for 3 h. Product was isolated using disposable PD 10 desalting columns following the instructions of the supplier and obtained as white powder (2.3 mg, 53%) after freeze drying.

For the synthesis of L17E-GFP11-dextran-TAMRA **22**, fresh stocks of ascorbic acid and $\text{CuSO}_4 \cdot 5\text{H}_2\text{O}$ in water were prepared. BTAA (6 eq. per N_3) was suspended in water, and $\text{CuSO}_4 \cdot 5\text{H}_2\text{O}$ (1 eq. per N_3) was added, yielding a dark blue solution, which decolorized after addition of ascorbic acid (3 eq. per N_3). In the meantime, L17E-Pra **15** (0.8 eq. per N_3) and alkyne-GFP11 **21** (0.8 eq. per N_3) were dissolved in DMSO and subsequently added to a solution of N_3 (5.4)-dextran-TAMRA **20** in sodium phosphate buffer (100 mM, pH 7.5). The aqueous solution of copper (I) was also added, yielding a final mixture of 10% (v/v) DMSO in 66 mM sodium phosphate buffer. The reaction was shaken for 2 h at 37°C and afterwards purified by consecutive analytical SEC-HPLC runs. The product-containing fractions were pooled and freeze-dried, yielding 7.4 mg (33%) as red solid.

The synthesis of GFP11-dextran-TAMRA **23** was realized by preparation of fresh stocks of ascorbic acid and $\text{CuSO}_4 \cdot 5\text{H}_2\text{O}$ in water. BTAA (7.2 eq. related to dextran **20**) was dissolved in water and $\text{CuSO}_4 \cdot 5\text{H}_2\text{O}$ (1.2 eq. per dextran **20**) was added, causing the solution to turn dark blue. After addition of ascorbic acid (3.6 eq. per dextran **20**), the solution decolorized. In the meantime, alkyne-GFP11 **21** (3.5 eq. related to dextran **20**) was dissolved in DMSO and added to N_3 (5.4)-dextran-TAMRA **20** in sodium phosphate buffer (100 mM, pH 7.5). The aqueous solution of copper (I) was also added, yielding a final mixture of 10% (v/v) DMSO in 66 mM sodium phosphate buffer. The reaction was shaken for 2 h at 37°C and afterwards purified by consecutive analytical SEC-HPLC runs. The product containing fractions were pooled and freeze-dried, yielding 3.6 mg as red solid.

2.26 | Synthesis of DEACM-OH 31

Synthesis was carried out according to a protocol modified from Zhang et al.³³ A solution of 7-diethylamino-4-methylcoumarin **30** (1.0 eq.) and selenium dioxide (1.04 eq.) in xylene was stirred at reflux for 48 h. The reaction mixture was allowed to cool to room temperature and filtered, and the solvent was removed under reduced pressure. The residue was dissolved in methanol, and sodium borohydride (0.9 eq.) was added. The solution was stirred for 4 h at room temperature, followed by addition of water and neutralization with 1 M HCl. The organic solvent was removed under reduced pressure, and the aqueous phase was extracted with DCM (5 × 100 ml). The combined organic layers were dried over MgSO₄, the solvent removed in vacuo, and the crude product was purified by column chromatography (DCM → DCM/acetone 1:1) to yield 1.92 g (43%) of the title compound.

2.27 | Synthesis of DEACM-pNP 32

DEACM-OH **31** (1.0 eq.) and 4-nitrophenyl chloroformate (2.0 eq.) were dissolved in DCM and cooled to 0°C. DIEA (2.0 eq.) was added, and the solution was stirred at room temperature for 12 h. The appearing precipitate was dissolved by addition of DCM, and the reaction mixture was stirred for an additional hour. The solvent was removed under reduced pressure, and the crude product was purified by column chromatography (DCM → DCM/acetone 10:1) to yield 1.53 g (53%) of the title compound.

2.28 | Synthesis of Fmoc-L-Lys (DEACM)-OH 33

DEACM-pNP **32** (1.0 eq.) suspended in DMF/DCM (1:1) was added to Fmoc-L-Lys-OH (0.97 eq.) suspended in toluene/DCM (3:2). The suspension was cooled to 0°C, and DIEA (1.0 eq.) was added. The reaction mixture was stirred for 12 h, while allowing to come to room temperature. DIEA (0.3 eq.) was added, and the solution was stirred for an additional hour. The solvents were removed under reduced pressure, and the crude product was purified by column chromatography (DMC/MeOH/AcOH 95:5:0.1). After lyophilization from dioxane, 1.12 g (87%) of the title compound was obtained.

2.29 | Cell culture

HeLa cell line was incubated under standard conditions at 37°C in a humidified incubator with 5% CO₂. Cells were grown in Dulbecco's Modified Eagle's Medium (DMEM) (Sigma Aldrich) with 10% fetal bovine serum (FBS) (Merck KGaA, Darmstadt, Germany) and 1 × penicillin/streptomycin (pen/strep) (Life technologies, Carlsbad, CA, USA). HeLa-eGFP654 cells were ordered from the UNC Tissue Culture facility (Chapel Hill, NC, USA).

2.30 | HeLa-GFP1-10

HeLa cells were seeded in a 12-well plate in a density of 5.5×10^4 cells/well and incubated for 24 h under standard conditions (in DMEM without pen/strep). The cells were transfected with pQCXIP-GFP1-10 plasmid³⁴ (Addgene plasmid #68715, gifted from Yutaka Hata) using *lipofectamine* 2000 (Invitrogen, supplier Thermo Fisher Scientific) following the instructions of the supplier. For the selection of stably transfected cells, the cells were treated 72 h after transfection with $0.5 \mu\text{g} \times \text{ml}^{-1}$ puromycin. The concentration of puromycin was increased stepwise over 2 weeks to a final concentration of $1.2 \mu\text{g} \times \text{ml}^{-1}$.

2.31 | Cellular uptake assay

HeLa cells were seeded in 8- or 18-well microscopy slides in a density according to manufacturer protocol and incubated for 24 h under standard conditions at 37°C in a humidified incubator with 5% CO₂ in a volume DMEM (+10% FBS) corresponding to the applied slide size. Cells were treated with the constructs in DMEM (w/o FBS) for 1 h under standard conditions at 37°C in a humidified incubator with 5% CO₂, washed with phosphate-buffered saline (PBS) twice, and incubated further 3 h in DMEM (+10% FBS) at 37°C and 5% CO₂. After washing with PBS, cells were fixed in 4% paraformaldehyde (15 min, ambient temperature).

For live-cell imaging of split-GFP assay, HeLa-GFP1-10 cells were seeded in eight-well microscopy slides in a density of 1.5×10^4 cells/well. After overnight incubation under standard conditions, the medium was aspirated and the cells washed twice with PBS. Serum-free DMEM was added, followed by the compounds (10 × concentrated in PBS). After incubation for 1 h, the supernatant was removed, and the cells were washed twice with PBS and further incubated for 24 h in DMEM (+10% FBS). Prior to microscopy, the medium was aspirated, and the cells were washed twice with PBS and finally covered in either PBS or Hank's solution (0.35 g/L NaHCO₃, with Ca²⁺, and Mg²⁺).

2.32 | Cell-viability assay

For assessment of cytotoxicity of construct **7** and L17E **8**, HeLa cells were seeded in a 96-well plate in a density of 1.5×10^4 cells/well in a volume of 90 μl serum free DMEM. Cells were incubated for 24 h under standard conditions at 37°C in a humidified incubator with 5% CO₂, and subsequently, a serial dilution of the construct in 10 μl PBS was added and cells incubated for 1 h at 37°C and 5% CO₂. After further 3 h incubation in DMEM (+10% FBS) at 37°C and 5% CO₂, cell viability was measured with a Tecan® (Männedorf, Switzerland) *Infinite F200 Pro* using CellTiter96® Aqueous One Solution Cell Proliferation Assay (Promega) following the instructions of the supplier.

Cytotoxic studies of construct **22** were performed with HeLa cells, seeded in a 96-well plate in a density of 1.0×10^4 cells/well in a

volume of 100 μ l DMEM (+10% FBS). After incubation for 24 h under standard conditions, the medium was aspirated, and the cells were washed twice with PBS. A total of 90 μ l serum-free DMEM were added, and a serial dilution of construct **22** in 10 μ l PBS was added. After incubation for 1 h at 37°C and 5% CO₂, the supernatant was removed, and the cells were washed twice with PBS. DMEM (+10% FBS) was added, and the cells were incubated for further 24 h, followed by measuring the cell viability using CellTiter96® Aqueous One Solution Cell Proliferation Assay.

2.33 | PNA mis-splicing correction assay

A total of 3×10^4 HeLa-eGFP654 cells/well in DMEM with 10% FBS were seeded in a 48-well plate and incubated at 37°C in a humidified incubator with 5% CO₂ overnight. Prior to treatment with construct **29** or thiol-PNA, the medium was removed, the cells were washed with PBS, and DMEM without L-glutamine, L-cystine, and L-methionine was added. Construct **29** in different concentrations (10 \times concentrated in PBS, pH 6) was added, and the cells were incubated for 30 min at 37°C. After removal of the supernatant, the cells were washed with PBS and subsequently with low-pH glycine buffer (cooled to 4°C). After an additional washing step with PBS, the cells were treated with DMEM containing 10% FBS and incubated at 37°C in a humidified incubator with 5% CO₂ for 24 h. After aspiration of the medium, cells were washed with PBS and trypsinized for 10 min, where after DMEM with 10% FBS was added. Cell suspensions were transferred to a 96-well round bottom plate and centrifuged. The supernatant was discarded, and the cells were resuspended in PBS and transferred to FACS tubes.

2.34 | Fluorescence-activated cell sorting (FACS)

Cell sorting was performed using the *Influx*™ (BD Bioscience, Heidelberg, Germany) cell sorter.

2.35 | Microscopy

Fluorescence microscopy was performed on a Zeiss Axio Vert A1 FL (Carl Zeiss AG, Jena, Germany) equipped with Axio Cam ICM1. GFP was detected with a $\lambda = 470$ nm laser, and TAMRA was excited at $\lambda = 540$ –580 nm. Confocal laser scanning microscopy was performed on a Leica TSC SP8 confocal microscope (Leica Microsystems CMS GmbH, Wetzlar, Germany).

2.36 | L17E-3PG **34** and L17E-5PG **35** uncaging studies

Removal of the photocleavable protecting groups was achieved by irradiation of a 10 μ M peptide solution in PBS buffer (pH = 7.0, Roche


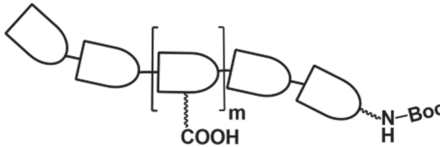
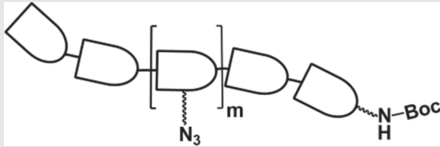
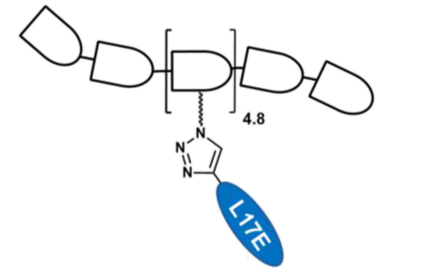
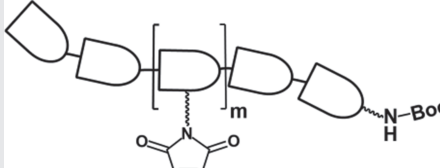
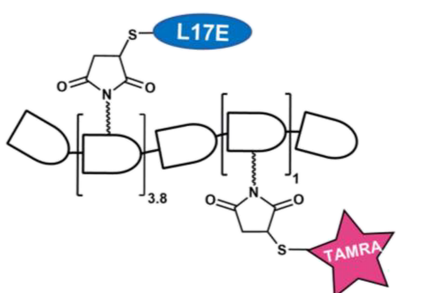
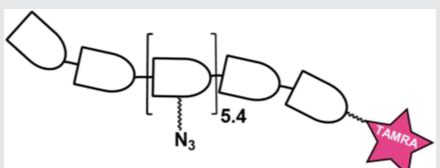
Diagnostics GmbH, Mannheim, Germany) with 10% DMSO at 405 nm in a stirrable QS semi-micro-cuvette from Hellma GmbH & Co. KG (Müllheim, Germany). As an irradiation source, an Osela inc. (Lachine, QC, Canada) Streamline Laser (405 nm, 100 mW, 70 mA) was used. Aliquots of 10 μ l were taken after 0, 10, 20, 40, 60, 90, 120, 180, 300, and 600 s; diluted to 100 μ l with water, and analyzed by UPLC and LC-MS.

3 | RESULTS AND DISCUSSION

3.1 | Dextran scaffold

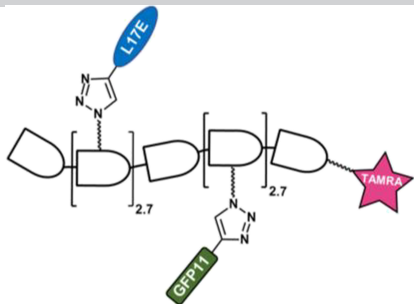
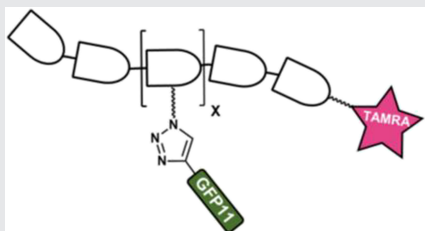
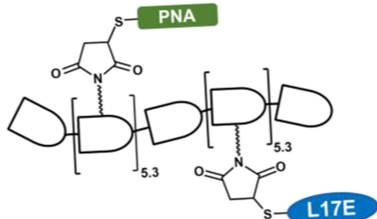


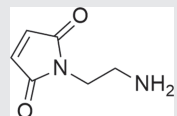
Comprising α -(1–6) glycosidic bonds between D-glucose repeating units,²⁸ dextran polysaccharide is a hydrophilic and biocompatible material.³¹ In this work, a 10 kDa dextran from the bacterium *Leuconostoc mesenteroides* was used, which shows only little branching of α -(1–3) linkages.³⁵ Recently, our group has reported the application of dextran as multivalent scaffold for the generation of antibody-drug conjugates with high drug-to-antibody ratio and improved hydrophilic properties.³¹ In a subsequent publication, we further demonstrated the potency of this polysaccharide as multimerization platform upon induction of tumor cell apoptosis by dextran decorated with multiple receptor-binding peptides.³² Herein, we designed a dextran-peptide hybrid bearing multiple L17E units. In accordance with our previous research, we derivatized both the hydroxy groups of the glucose repeating units and the reducing end to yield two orthogonal conjugation sites (Scheme 1A) to ensure a modular delivery system.^{31,32} The approach is based on the decoration of the repeating units with cargo and CPP in multiple copies stoichiometrically, which is a viable option for the payloads of moderate size, such as peptides or small molecules.²⁸ This allows for the delivery of multiple cargo molecules simultaneously (Scheme 1B), with an additional functionality placed at the reducing end. Dextran conjugates with different density of L17E peptide were synthesized applying copper-catalyzed version of Huisgen cycloaddition³⁶ or relying on thiol-maleimide chemistry. Thus, for cell cytotoxicity assay, peptide L17E was assembled by SPPS, and C-terminal alkyne was introduced by Fmoc-propargylglycine, yielding L17E derivative **1** (Table 1). Respectively, dextran was modified at the reducing end via reductive amination with *N*-Boc-cadaverine, followed by carboxyethylation at the glucose repeating units.²⁸ Subsequently, amide coupling of an azide linker yielded a multivalent construct **6** comprising on average 4.8 addressable azides per dextran unit. Copper-catalyzed alkyne-azide “click” yielded dextran-L17E hybrid **7** that was used to evaluate toxicity in cell-viability assays. For the evaluation of cell penetration using functional cargoes of diverse nature, conjugation was conducted upon modifications either at the reducing end of a polysaccharide or at its repeating units or by the combination of both approaches. To modify reducing end of dextran, reductive amination with *N*-Boc-protected cadaverine was applied, thus enabling an orthogonal coupling site for modification. All these issues will be further discussed in Section 3.3.

TABLE 1 Synthesized compounds

Compound	Description	Abbreviation in text
Dextran derivatives		
2		Dextran-N-Boc-cad
3 9 26		CE-dextran-N-Boc-cad 3: m = 4.8 9: m = 6.5 26: m = 10.5
6 19		N ₃ -dextran-cad 6: m = 4.8 19: m = 5.4
7		L17E(4.8)-dextran-cad
13 27		Maleimide-dextran-N-Boc-cad 13: m = 6.5 27: m = 10.5
16		TAMRA(1)-L17E(3.8)- dextran-N-Boc-Cad
20		N ₃ (5.4)-dextran-TAMRA

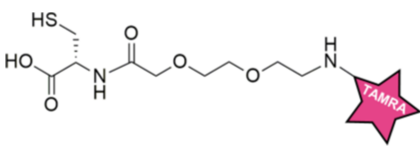
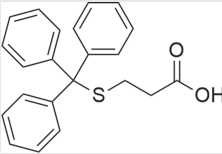
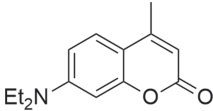
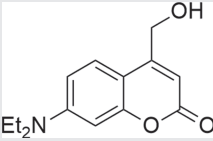
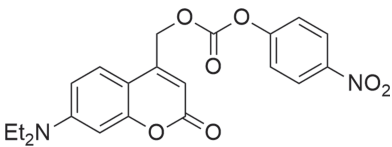
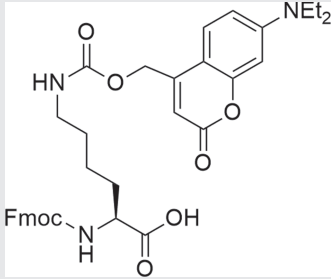
(Continues)

TABLE 1 (Continued)

Compound	Description	Abbreviation in text
22		L17E(2.7)-GFP11(2.7)-dextran-TAMRA
23		GFP11-dextran-TAMRA
29		L17E(5.3)-PNA(5.3)-dextran-N-Boc-cad
Peptides/PNA		
1	<i>H</i> -IWLTALKFLGHAAKHEAKQQLSKL-Pra-NH ₂	L17E-Pra
8	<i>H</i> -IWLTALKFLGHAAKHEAKQQLSKL-NH ₂	L17E
14	<i>H</i> -IWLTALKFLGHAAKHEAKQQLSKL-NH ₂	L17E-Cys
21		Alkyne-GFP11
24	<i>H</i> -RDHMLHEYVNAAGIT-NH ₂	GFP11
28		Thiol-PNA
34	<i>H</i> -IWLTALK ^{DEACM} FLGKHAAK ^{DEACM} H EAKQQLSK ^{DEACM} L-Pra-NH ₂	L17E-3PG
35	<i>H</i> -IWLTALK ^{DEACM} FLGK ^{DEACM} HAAK ^{DEACM} H EAK ^{DEACM} QQLSK ^{DEACM} L-Pra-NH ₂	L17E-5PG
Building blocks		
12		<i>N</i> -(2-aminoethyl) maleimide

(Continues)

TABLE 1 (Continued)

Compound	Description	Abbreviation in text
15		TAMRA-Thiol
25		S-Trityl-3-mercaptopropionic acid
30		DEACM
31		DEACM-OH
32		DEACM-pNP
33		Fmoc-L-Lys (DEACM)-OH

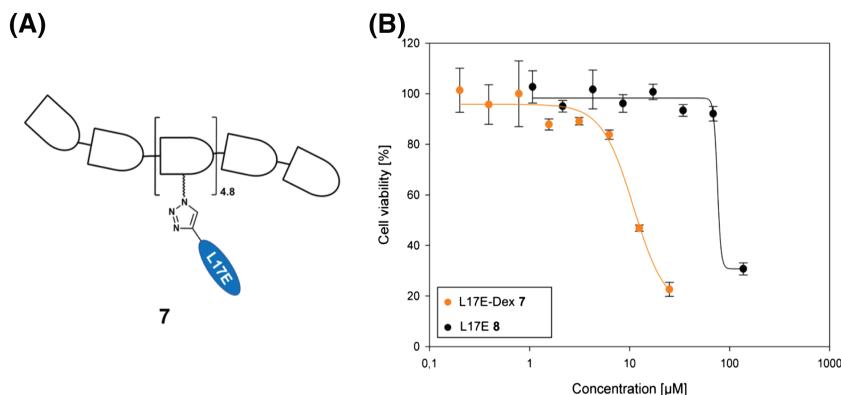
Note. Not mentioned are synthetic intermediates, which are given in the supporting information. Experimental details are discussed in the experimental part and in supporting information.

3.2 | Assessment of toxicity

Cytotoxicity of dextran-L17E hybrid **7** and solitary L17E **8** was studied in HeLa cells. It is interesting to note that L17E, being derived from naturally haemotoxic lycotoxin, possessed rather low toxicity in the taken cell line. Indeed, similar to Akishiba et al.,¹⁶ we did not observe a decrease in cell viability (Figure 1) when incubating HeLa cells with L17E peptide at high—up to 70 μM —concentrations. However, the hybrid module **7** bearing on average 4.8 L17E units, showed an IC_{50} value of approximately 10 μM , that corresponds to 48 μM solitary L17E. This roughly 1.5-fold increase in cytotoxicity could be caused

by multivalency effects, but the value is still in acceptable range. The cytotoxicity of TAMRA-labeled dextran hybrids is shown in Sections S1.1.2 and S1.2.2. Investigating cell viability in the presence of the construct possessing six L17E units per dextran molecule, we found that the toxicity increased to approximately 2.5 μM with the increasing density of peptide (Figure S4). On the other hand, in good accordance with this observation, the TAMRA-labeled construct **22** bearing only 2.7 L17E per dextran revealed moderate cytotoxicity up to 20 μM (Figure S11). Moreover, it is important to mention that TAMRA labeling could induce additional cytotoxicity as has been reported previously.³⁷

FIGURE 1 (A) Schematic depiction of L17E-dextran conjugate **7**, bearing 4.8 L17E per dextran on average, employed in cell viability assay on HeLa cell line. (B) Cell viability assay: HeLa cells treated with construct **7** and solitary L17E **8** for 1 h, followed by incubation in medium only for further 3 h



3.3 | Delivery of payloads using synthetic dextran-peptide hybrids

3.3.1 | Synthesis of TAMRA-labeled dextran-L17E conjugate

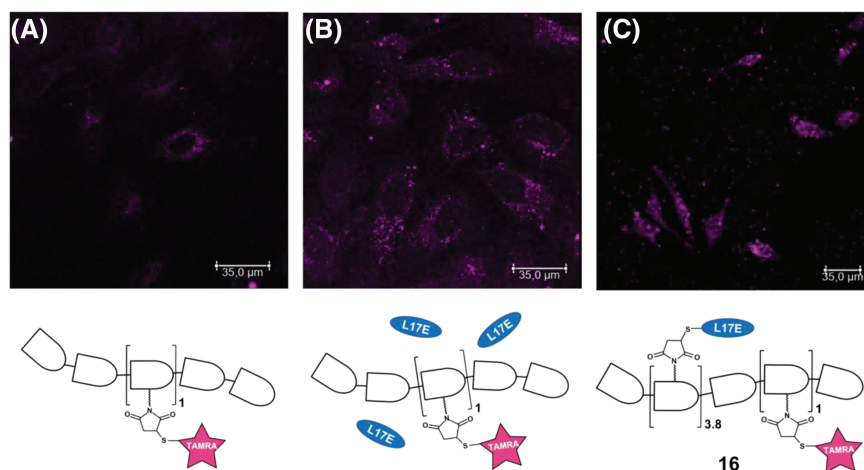
For validation of our modular strategy, delivery of different payloads was investigated. As a model for small molecules, we labeled our L17E-dextran hybrid with the fluorophore carboxytetramethylrhodamine (TAMRA). We first evaluated the ability of a fluorescently labeled dextran biomacromolecule equipped with multiple L17E peptide units to enter HeLa cells. To that end, we decorated a 10 kDa dextran scaffold with multiple conjugation sites as reported previously.³¹ A Boc-protected cadaverine was installed at the polysaccharide reducing end upon reductive amination resulting in compound **2** bearing a protected amine conjugation site. Next, compound **2** was modified with 6.5 carboxyethyl groups on average, via carboxyethylation of the hydroxylic groups at the C2 position of the glucose repeating units, giving dextran **9**. The resulting carboxylic moieties were addressed with *N*-(2-aminoethyl)maleimide **12** upon activation with *N*-ethoxycarbonyl-2-ethoxy-1,2-dihydroquinoline (EEDQ), giving dextran **13** equipped with 6.5 maleimide sites for subsequent conjugation of L17E peptide and TAMRA fluorophore by thiol-maleimide Michael addition.

For that purpose, an additional cysteine was introduced in the L17E sequence C-terminally, yielding peptide **14** after 9-fluorenylmethoxycarbonyl (Fmoc) SPPS. To obtain the ultimate TAMRA-labeled L17E-dextran, construct **13** was incubated with a stoichiometric mixture of 1 part of TAMRA-thiol **15** and 5.5 of L17E-Cys peptide **14** in MES buffer, resulting in dextran **16** equipped with TAMRA label and 3.8 L17E peptides on average.

3.3.2 | Delivery of TAMRA in HeLa cells

HeLa cells were treated in medium for 1 h with TAMRA-labeled dextran (10 kDa, 25 μM), TAMRA-L17E(3.8)-dextran **16** (3.13 μM), and for comparison with TAMRA-labeled dextran (10 kDa) coincubated with L17E peptide **8** (40 μM) according to Akishiba et al.¹⁶ After further 3 h incubation in medium only, the cellular distribution of the fluorescent constructs was analyzed by confocal laser scanning microscopy (CLSM). While cells treated with TAMRA-labeled dextran (10 kDa, 25 μM) in absence of L17E peptide only showed weak uptake of the macromolecule (Figures 2A and S1), cells coincubated with 40 μM L17E peptide, as expected, showed clearly enhanced uptake of TAMRA-labeled dextran (10 kDa, 25 μM) with signals of intense TAMRA fluorescence punctually distributed in the cytoplasm omitting the region of the nucleus (Figures 2B and S2). Cells treated

FIGURE 2 Fluorescence microscopy images of HeLa cells treated with different TAMRA-labeled dextrans. TAMRA-fluorescence channel. (A) TAMRA-fluorescent HeLa cells incubated with 25 μM TAMRA-labeled dextran. (B) TAMRA-fluorescent HeLa cells incubated with 25 μM TAMRA-labeled dextran plus 40 μM coincubation with solitary L17E. (C) TAMRA-fluorescent HeLa cells incubated with 3.13 μM compound **16**, TAMRA-labeled dextran, bearing 3.8 covalently conjugated L17E per dextran on average



with TAMRA-L17E(3.8)-dextran **16**, equipped with 3.8 covalently bound L17E peptide molecules on average, showed TAMRA fluorescence spread all over the cytosol and in the nucleus, already at 3.13 μM concentration (Figures 2C and S3). This finding encouraged us to apply the dextran scaffold with multiply attached L17E peptides as uptake-mediating module for intracellular delivery of conjugated cargo.

3.3.3 | Verification of cytoplasmic delivery

It was important to find an appropriate method to verify cytoplasmic or nuclear localization of the construct and exclude possible entrapment of the modified dextran in other cell compartments such as endosomes. To this end, the split green fluorescent protein (GFP)

complementation assay³⁸ was employed, based on the recombination of the fragment peptide GFP 11 with cytosolic protein GFP 1–10. The structure of GFP is defined by a beta barrel consisting of 11 β strands. In a split GFP complementation assay, a nonfluorescent version missing the C-terminal beta-strand (GFP 1–10) is functionally complemented by noncovalent assembly with the 16 amino acid peptide, GFP 11.³⁹ This assay has already been used for detection of cytoplasmic uptake of the GFP 11 fragment fused to CPPs, while the GFP 1–10 fragment was stably expressed in the cytosol of cells.³⁸ We synthesized dextran **19** bearing an average of 5.4 azide groups and coupled TAMRA to its reducing end (construct **20**). For introduction of GFP 11 and L17E, both peptides equipped with an alkyne functionality and GFP 11 with an additional GSSG linker (construct **21**) were conjugated in equimolar ratio via copper-catalyzed azide-alkyne cycloaddition (CuAAC; Figure S60) to yield construct **22** (Figure 3A). As control,

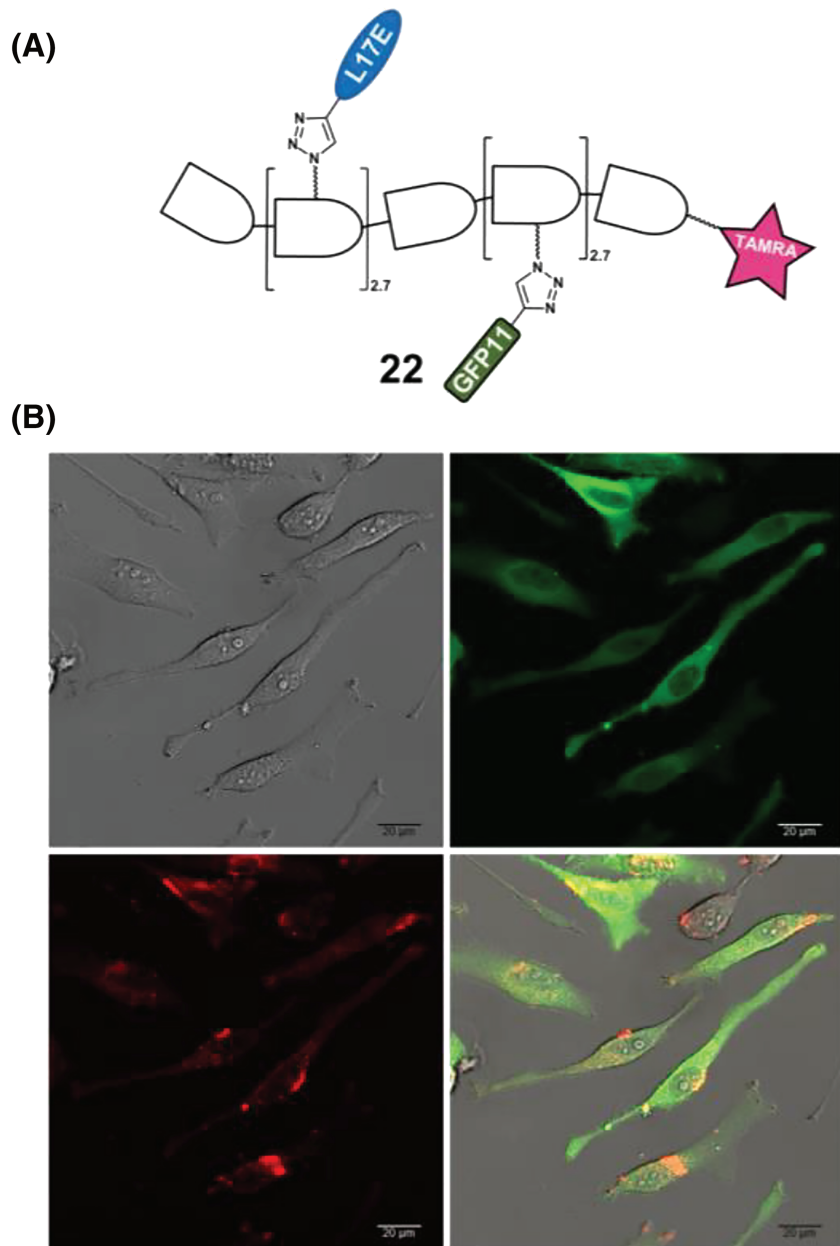


FIGURE 3 (A) Schematic depiction of dextran construct **22**. (B) Live-cell CLSM images (20x) of HeLa-GFP1–10 cells treated with 15 μM construct **22**, brightfield (top left), GFP-fluorescence channel (top right), and TAMRA-fluorescence channel (bottom left) and merge

TAMRA-dextran **20** bearing only GFP 11 peptide was also synthesized (construct **23**).

Stable transfected HeLa cells, expressing GFP 1–10 in the cytosol, were either coincubated with L17E-peptide **8** and GFP 11 peptide **24** or incubated with dextran **23** as control or **22** for 1 h in medium. After further 24 h incubation in medium, cells were analyzed with CLSM and FACS (Figure S12). Compared to cells coincubated with L17E and GFP 11 (Figure S9), HeLa-GFP 1–10 cells treated with construct **22** (Figures 3B and S5–S7) displayed distinctly higher GFP-fluorescence in a concentration-dependent manner. The control dextran hybrid **23** decorated only with GFP 11 shows no significant increase in GFP fluorescence (Figure S8) compared to cells treated with PBS, confirming that L17E is required for successful cellular uptake. However, since no significant difference between GFP 11 and L17E coincubation and PBS (Figures S9 and S10) was observed, we suggest that in this case covalent conjugation of both peptides to dextran is required for cytoplasmic uptake. Since the GFP 1–10-producing HeLa cells are a heterogeneous mixture of clones obtained by transfection and cell propagation, one can expect that not all of them express GFP 1–10, which may explain the finding that not all cells display functional GFP complementation (Figure 3B).

3.3.4 | Cellular uptake of PNA-loaded dextran-L17E hybrids

As a second approach to validate cytoplasmic delivery and even nuclear uptake, a mis-splicing correction assay with bioactive PNA was performed.⁴⁰ This assay is based on HeLa cells stably transfected with enhanced GFP (eGFP) gene, interrupted by a mutated intron. As a result of this point mutation, aberrant splicing sites are activated, leading to mRNA containing remains of the intron and therefore translation of

nonfunctional eGFP. Upon hybridization of an antisense oligonucleotide, for example, PNA or morpholinos,⁴⁰ to the mutated intron, the splicing is corrected and functional eGFP is produced. As a consequence, the amount of intracellular eGFP correlates with delivered PNA to the nucleus and can be relatively quantified using flow cytometry. In a slightly different setup, based on luciferase as reporter protein, this assay has already been used to study CPP-mediated delivery of PNA.^{9,41}

The required 18mer PNA was synthesized via manual Fmoc-SPPS with an additional C-terminal lysine for improved solubility. For subsequent conjugation to dextran, thiol **25** was introduced at the N-terminus of the PNA strand. Dextran **27** bearing an average of 10.5 maleimide functionalities at the repeating units on average and *N*-Boc cadaverine on the reducing end was decorated with thiol-PNA **28** and L17E-thiol **14** in equimolar ratio via Michael addition. HeLa-eGFP654 cells were incubated with construct **29** (Figure 4A) for 30 min in serum-free medium at 37°C, followed by further incubation in serum-containing medium for 24 h. Cells were trypsinized and subsequently analyzed by FACS (Figure S13). Cells incubated with L17E-PNA(10.5)-dextran conjugate **29** displayed higher fluorescence than untreated cells even at low concentration of 2.5 μM (Figures 4B and S13). Despite its large size of approximately 54 kDa and structural complexity, construct **29** was able to enter the nucleus, and the PNA could still hybridize to the mutated intron. The cellular uptake of thiol-PNA monomer **28** was investigated in a prior experiment, where no significant shift in fluorescence was observed (Figure S13).

3.4 | Photolabile masking of lysines to address polycation problem

The polycation dilemma is a common problem which persists for all types of drug classes and delivery systems. CPPs and other drug

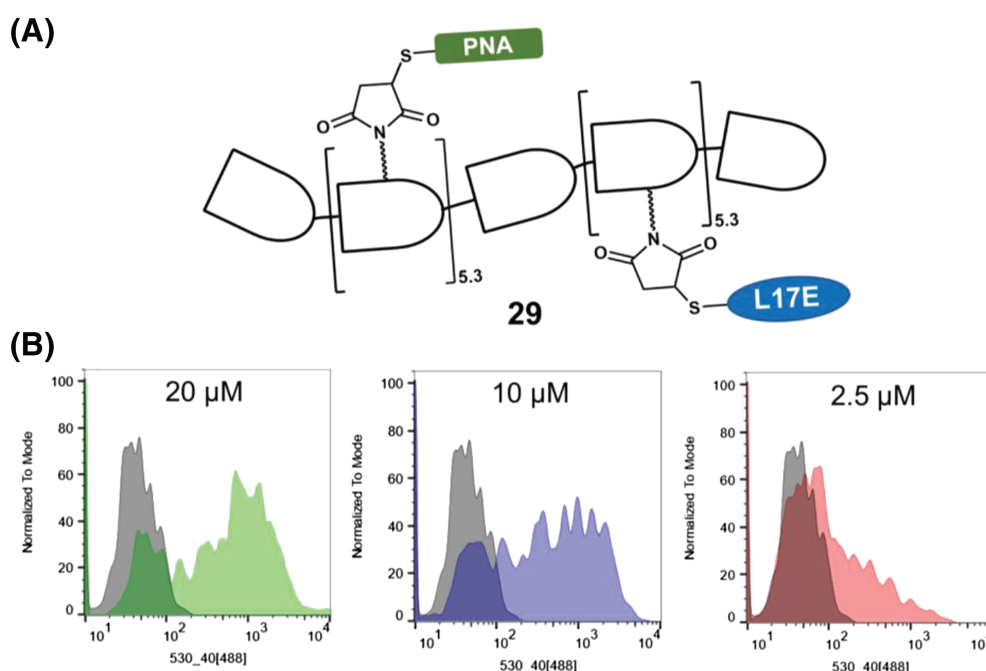


FIGURE 4 (A) Schematic depiction of L17E-PNA-dextran conjugate **29**. (B) FACS histograms (GFP-fluorescence on the x axis) of HeLa-eGFP654 cells treated with different concentrations of **29** (colored histograms) and PBS as control (gray histograms)

delivery systems utilizing their positive charge to interact with cell membranes often show promising performance *in vitro*, but the results *in vivo* may be disappointing. Independently of the administration route, whether oral or parenteral, their polycationic character is diminished by anionic mucosal membranes,⁴² serum albumin,⁴³ glycosaminoglycans,⁴⁴ and other polyanionic cell surface structures present on, for example, red blood cells,⁴⁵ on the way to the target site. To overcome these anionic barriers, strategies to mask the cationic sites with protecting groups until the target site is reached have been developed. These include pH-, redox- or enzyme-triggered systems, in which the underlying positive charge is unleashed under the unique conditions found in the tumor microenvironment.^{46–48} However, these systems are often insensitive and too slow to enable any accumulation around the tumor.^{47,49} A better alternative may be the application of physical stimulation of photoremovable protecting groups (PPGs) by light at the target site. Within the pool of PPGs, 7-diethylaminocoumarin (DEACM) has shown high deprotection efficiency by irradiation at 405 nm.^{24,25} In the present investigation, we used the highly efficient coumarin-based DEACM caging group to mask the positively charged lysine residues of L17E. The bathochromic shift introduced by the electron-donating groups at the C7 position results in an absorption maximum around 390 nm. In addition, the molecule displays a high quantum yield and an ultrafast release.^{50–53}

Following a procedure by Zhang et al.,³³ commercially available DEACM **30** was oxidized via Riley oxidation using SeO₂ to give the corresponding aldehyde. Subsequent reduction with NaBH₄ yielded alcohol **31**, DEACM-OH. Activation of the alcohol moiety was achieved by conversion into anhydride **32**, DEACM-pNP, with 4-nitrophenyl chloroformate. A nucleophilic attack by the ϵ -amino group of Fmoc-L-Lys-OH gave the desired SPPS building block **33**, Fmoc-L-Lys (DEACM)-OH.

The photocaged lysine derivative was incorporated into the sequence of L17E by standard Fmoc-SPPS. Two peptides were synthesized, bearing three (L17E-3PG **34**) and five (L17E-5PG **35**) cages, respectively. Uncaging studies were performed by irradiation of peptide solutions (10 μ M in PBS buffer at pH = 7.0 with 10% DMSO) at 405 nm and room temperature. Aliquots were analyzed by analytical RP-HPLC at 380 nm as a function of time. After 120 s, over 95% of the starting material had been consumed, and the fully deprotected L17E was identified via mass spectrometry (Figure S14). This fast and complete removal of the PPGs under irradiation was an encouraging first result. We found that protecting all five lysines with DEACM simultaneously results in a rather hydrophobic peptide, and we encountered solubility problems in PBS of the dextran polymer upon conjugation (data not shown). To date, it is unknown which of the L17E lysines are essential for cytoplasmic uptake. This issue is currently under investigation in our laboratory aimed at generating more water-soluble cell impermeable L17E variants, where only one or two lysines are DEACM protected, thus allowing for light-triggered cargo delivery.

4 | CONCLUSION

While a wealth of literature exists on the delivery of cargoes using arginine-rich peptides, comparably little is known about cellular passage relying on the arginine-lacking L17E variant of M-lycotoxin following a proposed novel uptake mechanism.²³ Indeed, no covalent cargo conjugates of this peptide have been reported to date. We developed a hybrid delivery system based on L17E peptide and dextran polysaccharide. Decoration of dextran with multiple L17E peptides led to a versatile module able to promote cytoplasmic delivery of covalently conjugated cargoes. As known from the literature,^{16,23} solitary L17E peptide was able to promote cytosolic uptake of proteins, up to full-length antibodies, upon simple incubation with the cargo. Having introduced a covalent bond between peptide and the cargo, combined with oligomerization on a dextran scaffold, we were able to generate polymer chimera that displayed cell cytoplasmic uptake at low concentration without compromising cell viability. It remains to be elucidated, whether the proposed uptake mechanism based on membrane ruffling also prevails for dextran-coupled L17E. The cytosolic delivery, promoted by the L17E-dextran module, was validated by split-GFP complementation assay, at which a cytosolically expressed GFP 1–10 protein fragment was complemented when the delivered GFP 11 cargo reached the cytosol and was not trapped in endosomes. Moreover, the L17E-dextran module was able to deliver bioactive peptide nucleic acids into the nucleus of HeLa cells, where the cargo PNA induced mis-splicing correction resulting in enhanced GFP fluorescence. This demonstrated the potential of dextran equipped with multiple L17E peptides to promote cytosolic and even nuclear uptake. Finally, we introduced the concept of L17E CPP lysine side chain photoprotection, which might allow for light induced-cargo delivery with possible ramifications for photodynamic therapy.

ACKNOWLEDGEMENTS

We thank Jan P. Bogen for his help with FACS analysis and Vanessa Reusche for sharing her expertise in peptide purification. We acknowledge financial support from the Deutsche Forschungsgemeinschaft (DFG) priority program SPP1623.

Open Access funding enabled and organized by ProjektDEAL.

ORCID

Harald Kolmar  <https://orcid.org/0000-0002-8210-1993>

REFERENCES

1. Tsomaia N. Peptide therapeutics: targeting the undruggable space. *Eur J Med Chem.* 2015;94:459–470.
2. Mitragotri S, Burke PA, Langer R. Overcoming the challenges in administering biopharmaceuticals: formulation and delivery strategies. *Nat Rev Drug Discov.* 2014;13(9):655–672.
3. Chapman AM, McNaughton BR. Scratching the surface: resurfacing proteins to endow new properties and function. *Cell Chem Biol.* 2016; 23(5):543–553.
4. Pei D, Buyanova M. Overcoming Endosomal entrapment in drug delivery. *Bioconjug Chem.* 2019;30(2):273–283.

5. Mastrobattista E, Koning GA, van Bloois L, Filipe ACS, Jiskoot W, Storm G. Functional characterization of an endosome-disruptive peptide and its application in cytosolic delivery of immunoliposome-entrapped proteins. *J Biol Chem.* 2002;277(30):27135-27143.
6. Kumar M, Gupta D, Singh G, et al. Novel polymeric nanoparticles for intracellular delivery of peptide cargos: antitumor efficacy of the BCL-2 conversion peptide NuBCP-9. *Cancer Res.* 2014;74(12):3271-3281.
7. Bartolami E, Basagiannis D, Zong L, et al. Diselenolane-mediated cellular uptake: efficient cytosolic delivery of probes, peptides, proteins, artificial metalloenzymes and protein-coated quantum dots. *Chemistry.* 2019;25(16):4047-4051.
8. Ruseska I, Zimmer A. Internalization mechanisms of cell-penetrating peptides. *Beilstein J Nanotechnol.* 2020;11:101-123.
9. Kauffman WB, Guha S, Wimley WC. Synthetic molecular evolution of hybrid cell penetrating peptides. *Nat Commun.* 2018;9(1):2568.
10. Jones SW, Christison R, Bundell K, et al. Characterisation of cell-penetrating peptide-mediated peptide delivery. *Br J Pharmacol.* 2005;145(8):1093-1102.
11. Liu J, Gaj T, Patterson JT, Sirk SJ, Barbas CF III. Cell-penetrating peptide-mediated delivery of TALEN proteins via bioconjugation for genome engineering. *PLoS ONE.* 2014;9(1):e85755.
12. Schneider AFL, Wallabregue ALD, Franz L, Hackenberger CPR. Targeted subcellular protein delivery using cleavable cyclic cell-penetrating peptides. *Bioconjug Chem.* 2019;30(2):400-404.
13. Dougherty PG, Sahni A, Pei D. Understanding cell penetration of cyclic peptides. *Chem Rev.* 2019;119(17):10241-10287.
14. Varkouhi AK, Scholte M, Storm G, Haisma HJ. Endosomal escape pathways for delivery of biologicals. *J Control Release.* 2011;151(3):220-228.
15. Qian Z, Martyna A, Hard RL, et al. Discovery and mechanism of highly efficient cyclic cell-penetrating peptides. *Biochemistry.* 2016;55(18):2601-2612.
16. Akishiba M, Takeuchi T, Kawaguchi Y, et al. Cytosolic antibody delivery by lipid-sensitive endosomolytic peptide. *Nat Chem.* 2017;9(8):751-761.
17. Li W, Nicol F, Szoka FC. GALA: a designed synthetic pH-responsive amphipathic peptide with applications in drug and gene delivery. *Adv Drug Deliv Rev.* 2004;56(7):967-985.
18. Tamemoto N, Akishiba M, Sakamoto K, Kawano K, Noguchi H, Futaki S. Rational design principles of attenuated cationic lytic peptides for intracellular delivery of biomacromolecules. *Mol Pharm.* 2020;17(6):2175-2185.
19. Herce HD, Schumacher D, Schneider AFL, et al. Cell-permeable nanobodies for targeted immunolabelling and antigen manipulation in living cells. *Nat Chem.* 2017;9(8):762-771.
20. Guo Z, Peng H, Kang J, Sun D. Cell-penetrating peptides: possible transduction mechanisms and therapeutic applications (review). *Biomed Rep.* 2016;4(5):528-534.
21. Jones AT, Sayers EJ. Cell entry of cell penetrating peptides: tales of tails wagging dogs. *J Control Release.* 2012;161(2):582-591.
22. Yan L, Adams ME. Lycotoxins, antimicrobial peptides from venom of the wolf Spider *Lycosa carolinensis*. *J Biol Chem.* 1998;273(4):2059-2066.
23. Akishiba M, Futaki S. Inducible membrane permeabilization by attenuated lytic peptides: a new concept for accessing cell interiors through ruffled membranes. *Mol Pharm.* 2019;16(6):2540-2548.
24. Klán P, Šolomek T, Bochet CG, et al. Photoremovable protecting groups in chemistry and biology: reaction mechanisms and efficacy. *Chem Rev.* 2013;113(1):119-191.
25. Menge C, Heckel A. Coumarin-caged dG for improved wavelength-selective uncaging of DNA. *Org Lett.* 2011;13(17):4620-4623.
26. Patel SG, Sayers EJ, He L, et al. Cell-penetrating peptide sequence and modification dependent uptake and subcellular distribution of green fluorescent protein in different cell lines. *Sci Rep.* 2019;9(1):6298.
27. Eggimann GA, Buschor S, Darbre T, Reymond J-L. Convergent synthesis and cellular uptake of multivalent cell penetrating peptides derived from Tat, Antp, pVEC, TP10 and SAP. *Org Biomol Chem.* 2013;11(39):6717-6733.
28. Richter M, Chakrabarti A, Ruttekkol IR, et al. Multivalent design of apoptosis-inducing bid-BH3 peptide-oligosaccharides boosts the intracellular activity at identical overall peptide concentrations. *Chem a Eur J.* 2012;18(52):16708-16715.
29. Chakrabarti A, Witsenburg JJ, Sinzinger MD, et al. Multivalent presentation of the cell-penetrating peptide nona-arginine on a linear scaffold strongly increases its membrane-perturbing capacity. *Biochim Biophys Acta.* 2014;1838(12):3097-3106.
30. Benjamin CJ, Wright KJ, Hyun S-H, et al. Nonfouling NTA-PEG-based TEM grid coatings for selective capture of histidine-tagged protein targets from cell lysates. *Langmuir.* 2016;32(2):551-559.
31. Schneider H, Deweid L, Pirzer T, et al. Dextramabs: a novel format of antibody-drug conjugates featuring a multivalent polysaccharide scaffold. *ChemistryOpen.* 2019;8(3):354-357.
32. Schneider H, Yanakieva D, Macarrón A, et al. TRAIL-inspired multivalent dextran conjugates efficiently induce apoptosis upon DR5 receptor clustering. *ChemBiochem.* 2019;20(24):3006-3012.
33. Zhang X, Xi W, Wang C, Podgórski M, Bowman CN. Visible-light-initiated Thiol-Michael addition polymerizations with coumarin-based photobase generators: another photoclick reaction strategy. *ACS Macro Lett.* 2016;5(2):229-233.
34. Kodaka M, Yang Z, Nakagawa K, et al. A new cell-based assay to evaluate myogenesis in mouse myoblast C2C12 cells. *Exp Cell Res.* 2015;336(2):171-181.
35. van Witteloostuijn SB, Pedersen SL, Jensen KJ. Half-life extension of biopharmaceuticals using chemical methods: alternatives to PEGylation. *ChemMedChem.* 2016;11(22):2474-2495.
36. Kolb HC, Finn MG, Sharpless KB. Click chemistry: diverse chemical function from a few good reactions. *Angew Chem Int Ed.* 2001;40(11):2004-2021.
37. Hedegaard SF, Derbas MS, Lind TK, et al. Fluorophore labeling of a cell-penetrating peptide significantly alters the mode and degree of biomembrane interaction. *Sci Rep.* 2018;8(1):6327.
38. Milech N, Longville BAC, Cunningham PT, et al. GFP-complementation assay to detect functional CPP and protein delivery into living cells. *Sci Rep.* 2015;5(1):18329-18329.
39. Cabantous S, Terwilliger TC, Waldo GS. Protein tagging and detection with engineered self-assembling fragments of green fluorescent protein. *Nat Biotechnol.* 2005;23(1):102-107.
40. Sazani P, Kang S-H, Maier MA, et al. Nuclear antisense effects of neutral, anionic and cationic oligonucleotide analogs. *Nucleic Acids Res.* 2001;29(19):3965-3974.
41. Shiraishi T, Nielsen PE. Peptide nucleic acid (PNA) cell penetrating peptide (CPP) conjugates as carriers for cellular delivery of antisense oligomers. *Artif DNA PNA XNA.* 2011;2(3):90-99.
42. Akkus ZB, Nazir I, Jalil A, Tribus M, Bernkop-Schnürch A. Zeta potential changing polyphosphate nanoparticles: a promising approach to overcome the mucus and epithelial barrier. *Mol Pharm.* 2019;16(6):2817-2825.
43. Dash PR, Read ML, Barrett LB, Wolfert MA, Seymour LW. Factors affecting blood clearance and in vivo distribution of polyelectrolyte complexes for gene delivery. *Gene Ther.* 1999;6(4):643-650.
44. Ziegler A, Seelig J. Interaction of the protein transduction domain of HIV-1 TAT with heparan sulfate: binding mechanism and thermodynamic parameters. *Biophys J.* 2004;86(1):254-263.
45. Fischer D, Li Y, Ahlemeyer B, Krieglstein J, Kissel T. In vitro cytotoxicity testing of polycations: influence of polymer structure on cell viability and hemolysis. *Biomaterials.* 2003;24(7):1121-1131.
46. Du J-Z, Sun T-M, Song W-J, Wu J, Wang J. A tumor-acidity-activated charge-conversional nanogel as an intelligent vehicle for promoted

- tumoral-cell uptake and drug delivery. *Angew Chem Int Ed*. 2010;49(21):3621-3626.
47. Kuai R, Yuan W, Qin Y, et al. Efficient delivery of payload into tumor cells in a controlled manner by TAT and thiolytic cleavable PEG co-modified liposomes. *Mol Pharm*. 2010;7(5):1816-1826.
48. Sun Z, Li R, Sun J, et al. Matrix metalloproteinase cleavable nanoparticles for tumor microenvironment and tumor cell dual-targeting drug delivery. *ACS Appl Mater Interfaces*. 2017;9(46):40614-40627.
49. Gao GH, Park MJ, Li Y, et al. The use of pH-sensitive positively charged polymeric micelles for protein delivery. *Biomaterials*. 2012;33(35):9157-9164.
50. Hagen V, Frings S, Wiesner B, Helm S, Kaupp UB, Bendig J. [7-(Dialkylamino)coumarin-4-yl]methyl-caged compounds as ultrafast and effective long-wavelength phototriggers of 8Bromo-substituted cyclic nucleotides. *Chembiochem*. 2003;4(5):434-442.
51. Herzig LM, Elamri I, Schwalbe H, Wachtveitl J. Light-induced antibiotic release from a coumarin-caged compound on the ultrafast time-scale. *Phys Chem Chem Phys*. 2017;19(22):14835-14844.
52. Shembekar VR, Chen Y, Carpenter BK, Hess GP. Coumarin-caged glycine that can be photolyzed within 3 μ s by visible light. *Biochemistry*. 2007;46(18):5479-5484.
53. van Wilderen LJGW, Neumann C, Rodrigues-Correia A, et al. Picosecond activation of the DEACM photocage unravelled by VIS-pump-IR-probe spectroscopy. *Phys Chem Chem Phys*. 2017;19(9):6487-6496.

SUPPORTING INFORMATION

Additional supporting information may be found online in the Supporting Information section at the end of this article.

How to cite this article: Becker B, Englert S, Schneider H, et al. Multivalent dextran hybrids for efficient cytosolic delivery of biomolecular cargoes. *J Pep Sci*. 2021;27:e3298. <https://doi.org/10.1002/psc.3298>